Interfacial delamination of a sandwich layer by aqueous corrosion

Sina Askarinejad[a], Vikram Deshpande[a], Norman Fleck[a,*]

[a]*Engineering Department, Cambridge University, Cambridge, CB2 1PZ, UK*

Keywords: Cathodic delamination, Free corrosion, Water attack, Diffusion, Aqueous corrosion, Adhesive joints

Abstract

The mechanism of aqueous delamination of a methyl methacrylate -based adhesive layer, sandwiched between two steel plates, is investigated by a systematic series of critical tests. These tests include starving the specimen of oxygen, varying the aqueous environment from de-ionised water to water with a high concentration of salt, and varying the mechanical constraint imposed by the sandwich. Sandwich construction starves the delamination crack tip of oxygen, and delamination occurs by water attack of the interface. In contrast, an adhesive coating on a steel substrate undergoes cathodic delamination when oxygen is present at the crack tip and the delamination crack is filled with salt water.

*Corresponding author
Email address: naf1@cam.ac.uk (Norman Fleck)

1. INTRODUCTION

Adhesive joints offer significant benefit over mechanical fasteners, such as bolts and rivets, in applications ranging from civil engineering construction and automotive to ship-building [1; 2; 3]. However, the durability of adhesive joints in a harsh environment such as salt water is a concern [4], and there is a need to understand the competing degradation mechanisms of an adhesive joint in order to ensure their safe and reliable design.

A limited number of experimental techniques have been developed in order to determine the dominant corrosion mechanism for a coating or sandwich layer. Fractography, along with X-ray Photoelectron Spectroscopy (XPS) and energy dispersive X-ray analysis (EDAX), can be used for a posteri investigation of a delaminated coating and adhesive joint. The scanning Kelvin probe has also been used to infer the electrical potential distribution in an electrolyte-filled delamination beneath a coating; this instrument provides evidence that cathodic delamination is operative for a coating with an electrolyte-filled debond [5; 6; 7; 8].

In contrast to a thin coating of adhesive on a steel substrate, adhesive joints are typically shielded from the presence of oxygen due to the closed nature of the joint [9; 10]. Consequently, the corrosion mechanism in a closed joint may differ from that of a thin coating. Destructive mechanical tests on double-cantilever beams, butt joints and single-lap shear joints are used to measure the loss of mechanical strength in the closed joint configuration due to the presence of a corrosive environment. However, the loss of mechanical strength provides only indirect information on the diffusion and reaction kinetics of water, oxygen and ions, and consequently these tests give limited insight into the mechanisms behind degradation of adhesive joints [11].

This paper presents an experimental characterisation of the degradation of a sandwich layer comprising two outer low carbon steel plates of grade EN10139, and a bonded core made from a methyl methacrylate (MMA)-based adhesive. First, possible mechanisms of aqueous corrosion are summarised for the delamination of steel/adhesive/steel

sandwich specimens. Experiments are performed to determine the corrosion mechanism and delamination rate as a function of specimen configuration, NaCl concentration and oxygen availability.

1.1. Competing mechanisms of delamination

At least three delamination mechanisms can exist at an adhesive/steel interface when exposed to salt water as shown in Fig. 1: (A) free corrosion [12], (B) cathodic delamination [13; 14], and (C) water attack by [15; 16; 17]. The first two mechanisms are based on the same half-reactions: the iron oxidation reaction

$$\mathrm{Fe} \rightarrow \mathrm{Fe}^{2+} + 2\mathrm{e}^{-} \tag{1}$$

or the equivalent reaction for oxidation to Fe^{3+}; and the oxygen reduction reaction

$$\mathrm{H_2O} + \frac{1}{2}\mathrm{O_2} + 2\mathrm{e}^{-} \rightarrow 2\mathrm{OH}^{-}\,. \tag{2}$$

In *free corrosion* (Fig. 1a), both half-reactions occur in close proximity at the adhesive/steel interface; the ferrous and hydroxide ions combine to form a precipitate of hydrated rust

$$\mathrm{Fe}^{2+} + 2\mathrm{OH}^{-} \rightarrow \mathrm{Fe(OH)_2}\,. \tag{3}$$

Dissolution of the Fe^{2+} generates local pitting of the steel substrate and a delamination crack advances in the hydrated rust layer once a critical thickness of hydrated rust has formed.

In *cathodic delamination* (Fig. 1b), oxygen reduction to OH^{-} occurs at the cathodic crack tip. Oxygen is transported to the crack tip through the water-filled delamination and/or the polymer layer. Iron oxidation takes place at an anodic region remote from the delamination crack tip, such that the cathode and anode are widely separated. Electrons flow through the steel from the anodic, oxidation region of reaction (1) to the cathodic, reduction region of reaction (2). The production of OH^{-} at the crack tip establishes a highly alkaline environment within the delamination and this generates a passivating oxide layer on the steel surface. The local concentration of OH^{-} in the

water-filled delamination is balanced by an equal concentration of cations such as Na^+ for charge neutrality [18]. A negligible concentration of Cl^- diffuses along the defect to the delamination tip due to the adverse electric field [19; 20]. These features have been confirmed by local Auger spectroscopy [13]. The precise reactions that cause crack growth in cathodic delamination remain a matter of debate, and are dependent upon the polymer and iron oxide chemistries. For example, hydroxyl ions produced by oxygen reduction can destroy iron–oxygen–polymer bonds at the interface by hydrolysation or saponification [21]. More recently [14], it has been shown that short-lived intermediates exist during oxygen reduction, and these are more destructive to the interface than OH^-. In any case, the loss of adhesion is directly linked to the reduction of oxygen to OH^- and to the generation of intermediates at the metal/polymer interface.

The established literature suggests that the rate-limiting step of cathodic delamination is the migration of charge-balancing cations such as Na^+ in the electrolyte-filled delamination to the crack tip from a remote reservoir (sea water, for example) [14]. Assume that the delamination velocity $\dot{\ell}$ scales with the flux of cations along the delamination, and also assume that this flux is proportional to the gradient of electrochemical potential of cations over the delamination length, ℓ. Then, the delamination length scales with the square root of time, t. At a sufficiently low value of oxygen concentration, the rate limiting step switches to the tip kinetics of OH^- production [10; 22] and the parabolic dependence of delamination length with time may not occur. Very recently, the above viewpoint has been challenged by Khayatan and Rohwerder [23]: they suggest that the rate determining step in cathodic delamination is the insertion of cations into the cation-free intact interface. They assume that cation migration can occur along the surface of the metallic substrate with local charge balance achieved by surface charging (by electrons) of the substrate rather than bulk OH^- anions within the delamination. They also conclude that the importance of this delamination mechanism for delamination resistant coatings is the object of current research. In summary, cathodic delamination has the following characteristics: (i) a cathodic reaction exists at the delamination tip, and this is commonly oxygen reduction, (ii) an alkaline

electrolyte must be present within the delamination crack, and (iii) the established literature explains that cation diffusion within the electrolyte commonly dictates the rate of delamination and ℓ scales with $t^{1/2}$.

The third mechanism is *water attack* such that delamination is a result of water ingress in the interphase layer between the steel and adhesive (Fig. 1c). The presence of oxygen at the crack tip, and of an electrolyte within the delamination, play a negligible role. The precise details of the chemical reaction are unknown but possibilities have been discussed recently for water at the PMMA/aluminium oxide interface [24]. One possiblity is that hydrogen bonds between the metallic oxide and the carbonyl group of PMMA, that lead to adhesion, are replaced by water. The above three possible delamination mechanisms are summarized in Table 1 and the observable signatures corresponding to these competing delamination mechanisms are described in Table 2.

1.2. Objective of Study

The primary objective of this study is to elucidate the operative mechanisms of interfacial delamination for a methyl methacrylate -based adhesive layer, sandwiched between two steel plates, and for a steel plate with a thin coating of methyl methacrylate -based adhesive. The sensitivity of delamination rate to environment and to geometry is determined in a quantitative manner, and fractography is used to shed light on the active corrosion mechanisms. All tests are performed at room temperature of 20 °C, and a relative humidity of 50%. A sequence of 5 experiments are implemented, and are listed as follows. The intent is to make logical deductions on the active delamination mechanisms from the results of all 5 sets of experiments, when taken together.

- *Reference Experiment I*, to show that MMA-coated steel undergoes cathodic delamination.
- *Reference Experiment II*, to show that a steel/MMA/steel sandwich specimen delaminates by water attack.

- *Sensitivity Experiment III*, to determine the sensitivity of delamination of steel/MMA/steel sandwich specimens to oxygen concentration.
- *Sensitivity Experiment IV*, to determine the sensitivity of delamination of sandwich specimens to mechanical constraint.
- *Sensitivity Experiment V*, to determine the sensitivity of delamination of MMA-coated steel to oxygen concentration.

2. MATERIAL AND METHODS

2.1. Materials

A methyl methacrylate (MMA)-based adhesive, Scigrip®-300 [1], comprises a resin and a peroxide-based activator paste ($C_6H_5COO(-)$). The resin contains MMA monomers $C_5H_8O_2$, amines RNH_2 and additional rubbers and toughening agents. When the resin and activator are mixed, the peroxide reacts with the amines to release reactive free radicals. The free radicals react with a carbon-carbon double bond in the MMA monomers to give a rapid exothermic polymerization reaction. The chemical interaction between low carbon steel and Scigrip® is complex and is not detailed in the literature. In the present study, the MMA adhesive is bonded to a low carbon steel EN10139: DC01/CS4-C590. We emphasise that Scigrip®-300 is a compliant gap-filling adhesive with a Young's modulus of 300 MPa, in contrast to the engineering polymer PMMA which possess a Young's modulus on the order of 3.0 GPa.

2.2. Methods

Reference Experiment I: **MMA-coated steel specimen.** In order to evaluate the delamination of a thin layer of the MMA adhered to a low carbon steel substrate, the following material system was used. A steel shim of thickness 0.2 mm was cut to rectangular samples of 70 mm×35 mm and used as the substrate material, see

[1] https://www.scigripadhesives.com

Fig. 2. All steel samples were cleaned thoroughly by acetone to remove any possible contamination, and a coating of MMA adhesive, with a debond (defect) at one end of the coating, was applied to the steel substrate, as follows. First, PTFE tape was used to mask off an end strip of width 15 mm on the top face of the steel shim, as shown in Fig. 2a. Second, a coating of MMA adhesive, of thickness 100 µm, was applied to the top of the PTFE tape and to the exposed steel surface (Fig. 2b), and then, after a 72 hour room temperature cure, the coating was peeled off the PTFE tape but kept intact on the steel surface, see Fig. 2c. A defect was thereby produced. Finally, containment walls in the form of an epoxy[2] dam [10] were added and the defect was filled with an aqueous electrolyte, see Fig. 2d. The electrolyte was a NaCl solution of concentration 0.06 M, 0.6 M, and 3 M. The reference liquid of de-ionised (DI) water (0 M) was also employed.

The degree of delamination of the adhesive coating due to electrolyte exposure was measured by bending back the coating manually after selected times t, and then observing the delamination via an optical microscope. The delamination length $\ell(t)$ was the average value over at least 3 specimens. Error bars are included in the plots of $\ell(t)$ in the results section below to show the variability between specimens. The peeling operation to measure $\ell(t)$ is destructive and so, in order to generate a curve of delamination length ℓ versus time t, approximately 30 specimens were tested for each electrolyte.

Reference Experiment II: **MMA-steel sandwich specimens.** Steel/adhesive/steel sandwich specimens with an adhesive layer thickness of 0.8 mm and steel shims of thickness 0.2 mm were fabricated with no pre-crack. The specimens were rectangular and of dimension 50 mm×50 mm in plan view, as shown in Fig. 3a. In order to assess the effect of water on the durability of these specimens, they were submerged to a depth of 5 mm in salt water (0.6 M NaCl) or in de-ionized water. After immersion, the delamination lengths on each side of the specimen (ℓ_1 through ℓ_4, see Fig. 3a) were measured

[2]Araldite® Rapid, https://www.go-araldite.com

via an optical microscope by bending back the steel shim. As for the MMA-coated steel specimens, the bending operation is destructive and at least three identical specimens were used for each state of exposure. We define ℓ as the average of ℓ_1 through ℓ_4, over at least 3 specimens, and we again include error bars to show the variability between specimens.

Sensitivity Experiment III: **Sensitivity of delamination of sandwich specimens to oxygen concentration.** Free corrosion and cathodic delamination are both precluded in the absence of oxygen leaving water attack as the only available delamination mechanism. Consequently, if the delamination rate of a sandwich specimen is insensitive to the presence or absence of oxygen, then this suggests that water attack is the active delamination mechanism. In order to investigate the sensitivity of delamination rate of sandwich specimens to oxygen concentration, we performed delamination experiments on MMA sandwich specimens in a nitrogen chamber (with oxygen absent), at a flow rate of 0.2 litres of nitrogen per minute. The results were then compared to those of Experiment II which were conducted in an air atmosphere.

Sensitivity Experiment IV: **Sensitivity of delamination of sandwich specimens to mechanical constraint.** The coated specimens allow for the existence of a diffusion path for oxygen from the free surface of the coated specimen, through the thickness of the adhesive, and down to the interface. This path is not available for the sandwich specimen. But there is an additional difference: the presence of steel substrates of high bending stiffness in the sandwich specimen may reduces the opening of the delamination crack, and thereby reduce the amount of salt water that reaches the crack tip and thereby reduce the delamination rate. In order to assess the significance of the bending stiffness of the outer layers of the sandwich specimen, and thereby assess the relative significance of these two differences, the 0.2 mm thick upper steel facesheet of a steel/adhesive/steel sandwich joint was replaced by an aluminium foil of thickness 30 µm (Fig. 3b), and the evolution of delamination length of the adhesive/steel interface was measured as a function of time. The flexural stiffness of the aluminium foil is approximately three orders of magnitude less than that of the steel upper sheet

of the sandwich specimen. Thus, the Al foil imposes minimal additional mechanical constraint to that of the MMA-coated steel specimen, but inhibits the flux of oxygen from the top surface of the adhesive to the crack tip in a similar manner to that of the steel/adhesive/steel sandwich specimen.

Sensitivity Experiment V: **Sensitivity of delamination of MMA-coated steel to oxygen concentration.** This experiment is designed to test the following hypothesis: is the delamination response of adhesive-coated steel specimens, but starved of oxygen, equal to that of sandwich specimens in all aqueous environments? To investigate this, we conducted delamination tests on MMA-coated steel specimens in a nitrogen atmosphere and in-vacuo (200 mbar air pressure) following the protocol of Experiment I. The results will be compared with those of Experiment I in order to assess the sensitivity of delamination rate to oxygen concentration.

3. RESULTS

The results of the 5 sets of experiments is reported in turn. A summary of the associated fractography is then presented in order to note the fracture surface appearance due to each corrosion mechanism.

Reference Experiment I: **MMA-coated steel specimens.** The delamination length ℓ versus time t for a sequence of tests is plotted in Fig. 4a. Delamination is rapid in the presence of NaCl, and we shall now infer that delamination is due to cathodic delamination. The main indicators of this mechanism are: (i) the delamination rate increases with the NaCl concentration in the water; (ii) an alkaline environment (high pH level) exists inside the delamination crack; (iii) there is no sign of rust on the delaminated steel surface, and (iv) when transport of cations along the delamination to the crack tip is the rate limiting step, the delamination length is proportional to square root of time. We proceed to discuss whether these signatures of cathodic delamination are observed for the MMA-coated steel specimens.

Measurements of the delamination length versus time are included in Fig. 4a for a range of NaCl concentrations on a log-log scale. The delamination rate increases

with NaCl concentration, and the delamination length ℓ scales with the square-root of time t. This suggests that the transport of Na^+ cations from the defect (reservoir) along the interface is the rate-limiting step [14] in the delamination process. A full range pH indicator[3] solution was used to measure the pH of the liquid within the delamination. First, the electrolyte inside the reservoir was extracted to avoid mixing with the electrolyte inside the crack, and second, the thin adhesive layer was lifted and liquid pH indicator was applied to the liquid inside the crack. The colour of the liquid inside the crack indicated a pH value of 12 (for NaCl of concentration 0.06 M to 3M), as established by calibrations using 0.005 M NaOH and 1 M NaOH solutions. Note that the pH of the NaCl solutions in the reservoir was approximately 7. Finally, the delaminated surfaces in the presence of salt water showed no signs of pitting. All these observations suggest that cathodic delamination took place.

As shown in Fig. 4a, if de-ionised (DI) water is used, the delamination rate reduces significantly and the scaling of ℓ with time switches to linear suggesting that the delamination rate is dictated by the kinetics of the tip reaction. The absence of an electrolyte within the delamination implies that cathodic delamination is inactive. The full range pH indicator solution revealed that the liquid inside the crack had a pH value of 7, and the delaminated surfaces showed no signs of pitting. It is concluded that water attack is active rather than cathodic delamination or free corrosion.

Reference Experiment II: **MMA-steel sandwich specimens.** The measured delamination length ℓ versus time t characteristic of sandwich specimens exposed to salt water (0.6 M NaCl) and DI water is shown in Fig. 4b. The delamination rate is insensitive to the salt concentration of the aqueous solution and is very similar to the delamination rate in the MMA-coated steel specimens exposed to DI water, with ℓ increasing linearly with time t. This suggests that cathodic delamination is not the operative mechanism and the rate-limiting step is not the transport of species (such as Na^+, OH^-, oxygen or water) over the delamination length. Rather, the data suggest

[3]Fisher Chemical™, Thermo Fisher Scientific, Loughborough, UK

that the delamination rate is set by the rate constant of the reaction at the crack tip that induces delamination. Pitting is absent from the vicinity of the delamination tip, and this suggests that delamination is by water attack rather than by free corrosion. Additional support for this conclusion is given by the results of Experiment III, as now reported.

Sensitivity Experiment III: **Sensitivity of delamination of sandwich specimens to oxygen concentration.** The measured delamination rates in both DI and salt water and a nitrogen atmosphere (with oxygen absent) are plotted in Fig. 4b, along with the results for the sandwich specimens in air from Experiment II reported above. The delamination rates, to within experimental scatter, are identical in DI and salt water, regardless of the choice of ambient atmosphere, whether air or nitrogen. This suggests that an insufficient concentration of oxygen exists at the delamination tip to contribute to the corrosion mechanism, even for sandwich specimens tested in an air atmosphere. Thus, water attack is the dominant mechanism rather than free corrosion or cathodic delamination. The insensitivity of rate to salt concentration is additional evidence that water attack occurs rather than cathodic delamination.

Sensitivity Experiment IV: **Sensitivity of delamination of sandwich specimens to mechanical constraint.** The delamination length ℓ versus time t response is shown in Fig. 5, for specimens that contained an aluminium foil top layer, and were placed in DI water or in 0.6 M NaCl solution. The response of steel/adhesive/steel sandwich specimens are included in Fig. 5, and all tests were conducted in ambient air. The $\ell(t)$ characteristic is invariant, to within scatter, regardless of the choice of top layer (steel sheet or aluminium foil), and regardless of the choice of environment (DI water or salt solution). The interpretation is as follows. For both choices of top layer of sandwich specimen (steel sheet or aluminium foil), the opening of the delamination crack is sufficient for water to be present at the delamination tip and to induce delamination by water attack. The presence of Na^+ in the water-filled delamination crack has a negligible effect upon the mechanism of water attack. It is also concluded that the reduced delamination rate of a steel/adhesive/steel sandwich in aerated salt water,

compared to that of an adhesive-coated steel (see data of Fig. 4a re-plotted in Fig. 6) is due to the presence of the oxygen-impermeable top layer (steel or aluminium), and not due to the reduced oxygen supply associated with clamping shut of the water-filled delamination by the stiff steel substrates. As an aside, observations of the fracture surface for the 4 cases reported in Fig. 5 show that, to within 1 mm of the delamination tip, there is no evidence of rusting and pitting associated with free corrosion, again reinforcing the hypothesis that the tip is oxygen-starved.

Sensitivity Experiment V: **Sensitivity of delamination of MMA-coated steel to oxygen concentration.** Delamination tests on MMA-coated steel specimens were conducted in a nitrogen atmosphere and in-vacuo (200 mbar air pressure) following the protocol of Experiment I. The main trends from these results are clear from Fig. 7: an atmosphere of nitrogen, or a vacuum, reduces the delamination rate to that noted previously for the steel/adhesive/steel specimens (to simplify the presentation of the sandwich data from Fig. 4b, a best fit to these data is performed and is included as a single curve in Fig. 7). Further, note that the delamination rate of the MMA-coated steel is insensitive to salt concentration when oxygen is absent. We conclude that, by starving the adhesive coated steel specimens of oxygen, the delamination mechanism switches from cathodic delamination to water attack.

Fractography Representative examples of the fracture surface due to each corrosion mechanism are shown in Fig. 8, taken from particular experiments of the present study, and summarised as follows. For reference purposes, a scanning electron microscope (SEM) image of the surface of the steel of the present study is shown in the as-received state in Fig. 8a. In order to determine the effect of free corrosion on the appearance of the steel surface, steel samples were immersed in 0.6 M NaCl solution, and in de-ionised (DI) water, for 24 hours at room temperature (20 °C). Representative SEM images of the corroded steel surface (free corrosion) are shown in Fig. 8b after immersion in 0.6 M NaCl solution and in Fig. 8c after immersion in DI water. Pitting is evident in both cases. An example of the fracture surface resulting from cathodic delamination in Experiment I is given in Fig. 8d. This surface is a result of delamination of an MMA

adhesive coating (of thickness 100 µm) from the steel substrate, in an environment of 0.6 M NaCl solution at 20 °C. Neither pitting nor rusting is visible at the crack tip. It has been argued in the results of Experiment V that delamination of an MMA adhesive coating on a steel substrate occurs by water attack when oxygen is absent from the crack tip. For example, a 100 µm thick coating of MMA adhesive on a steel substrate delaminates by water attack when the delamination is fed by de-ionised water and the surrounding environment is nitrogen gas at 20 °C, with oxygen absent. The fracture surface for this mechanism is shown in Fig. 8e and is similar in appearance to that shown in Fig. 8d, with neither pitting nor rusting.

4. DISCUSSION

Cathodic delamination requires oxygen, water and cations to be present at the crack tip. The observed sensitivity of delamination rate to salt concentration in Experiment I for the MMA-coated steel specimens implies that cathodic delamination takes place in these specimens. The MMA adhesive coated steel specimen fails by cathodic delamination when the delamination contains an electrolyte such as salt water, and oxygen is available at the crack tip, recall Experiment I. In contrast, when DI water is used instead of salt water, the delamination rate of the adhesive coated steel drops dramatically, and the delamination characteristic $\ell(t)$ switches from a square-root dependence to a linear dependence, recall Fig. 4a.

The insensitivity of delamination rate to salt concentration in the sandwich specimens of Experiment II suggests that delamination is due to water attack (recall Table 2). Further, the delamination rate of the adhesive coated steel in DI water equals that of a steel/adhesive/steel sandwich specimen in DI water and equals that of a steel/adhesive/steel sandwich specimen in salt water (Fig. 4b). This is due to water attack being the delamination mechanism in both cases.

The present study reveals that aqueous corrosion of closed adhesive joints in the form of sandwich specimens occurs by water attack rather than cathodic delamination or free corrosion. A series of experiments have been performed in order to support this

conclusion. The logical development of the 5 sets of experiments and the conclusion from each are summarised in Table 3. The delamination length scales linearly with time for water attack, and scales with the square root of time for cathodic delamination (assuming that the rate limiting step for cathodic delamination is cation diffusion along the delamination rather than a tip reaction). Although the characteristics of cathodic delamination are established in the literature [19; 14], the characteristics of water attack are less well-documented [10; 16]. In particular, the feature of constant delamination velocity for water attack is of major practical significance in engineering design and certification[4] but is unclear from the literature.

The precise pathway for water migration to the delamination tip has not been identified in the present study. Water can diffuse through the adhesive and also migrate by capillary action along the delamination to the delamination tip. Water can also directly attack the tip of the delamination. These pathways are also available for the initiation of delamination at the free exposed edge of an adhesive/steel interface: water can diffuse to the interface through the adhesive, or can directly attack the interface at the free edge.

Three previous studies on closed joint configurations [9; 10; 25] exist in the literature where delamination length versus time $\ell(t)$ characteristics are reported. These data are re-plotted in Fig. 9 using logarithmic axes in order to determine whether a power law relation for $\ell(t)$ holds, and if so, the value of the exponent. Before summarising the details of the three cases, the overall conclusion is immediate: the data reveal a linear relation for $\ell(t)$.

Sorenson et al. [25] measured the delamination of a 300 µm thick epoxy coating on a low carbon steel substrate, and sealed the top of the adhesive coating by a 15 µm thick aluminium foil. The delamination was fed by a reservoir of 0.5 M KCl. Van Dam et al. [9] performed static wedge tests on double cantilever beams (arms of height 1.9 mm) made from an S690 low-alloy steel, and an epoxy adhesive (Araldite 2015) sandwich

[4] https://www.interreg2seas.eu/nl/qualify

layer of thickness 700 µm. The specimens were immersed in 0.6 M NaCl solution, and displayed two regimes of crack growth: an initial regime of stress-driven rapid growth, and a second regime of corrosion-driven slow growth during 100-700 hours of exposure. The data reported in Fig. 9 of the present study are taken from the data of Van Dam et al. [9] for 180-grit polished specimens, which is taken to be representative.

Andreon et al. [10] used a 30 µm thick borosilicate glass sheet instead of aluminium foil in order to provide a barrier to ingress of oxygen into their adhesive coated, DC04-steel specimens. The 30 µm thick adhesive coating was a water-dispersion polymer based on acrylic ester/styrene (Acronal®S 790 from BASF), and the delamination was fed by a reservoir of 0.5 M NaCl. They measured the delamination of an acrylic ester/styrene adhesive between a borosilicate glass thick foil and a steel plate, in a saltwater environment. They used a Scanning Kelvin Probe (SKP) and found that a potential gradient exists along the delamination, implying that a galvanic current exists with the outward flow of OH^- and the inward flow of cations such as Na^+. Thus, cathodic delamination occurs. However, the delamination rate is insensitive to the choice and concentration of cation in the electrolyte. This suggests that the rate limiting step is the reaction kinetics at the delamination tip rather than the transport kinetics of the cation Na^+ within the delamination to the crack tip.

Andreon et al. [10] also deduced that parabolic kinetics exist for the delamination rate, based on a plot of total delamination length versus time. An alternative interpretation of their data is as follows. The specimens of Andreon et al. [10] comprise two portions: (i) a region I of adhesive in the form of a coating (debonded from the steel substrate), with the feature that oxygen is able to migrate freely through the coating, and (ii) a region II of adhesive in the form of a sandwich layer between the glass foil and steel plate, such that oxygen transport can only occur in-plane within the adhesive layer, and not through the protective glass foil. Consequently, the relevant delamination length over which oxygen diffuses is that portion beneath the glass foil, and it is this reduced portion that is plotted in Fig. 9 of the present study. The replot of the data of Andreon et al. [10] in Fig. 9 of the present study suggests linear rather than

parabolic kinetics; linear kinetics are expected when the rate limiting step is a reaction at the delamination tip rather than the diffusion of oxygen along the delamination. In summary, it is argued here that the slow cathodic delamination of the sandwiched acrylic ester/styrene adhesive layer in a salt solution is due to the fact that the rate limiting step is the tip kinetics at low oxygen concentration.

The data shown in Fig. 9, when taken together, support the conclusion that the delamination velocity is almost constant for each material system, despite the wide range of adhesives, crack lengths and electrolytes employed. It is remarkable that the delamination velocities are similar given the wide range of materials and test methods. It is now argued that the delamination is either by water attack or by the autoreduction of Fe^{3+} oxide to Fe^{2+} oxide in the presence of water but oxygen absent [10; 22]. The autoreduction reaction, as proposed by Wint et al. [26], is of the type

$$Fe_2O_3 + 3H_2O + 2e^- \rightarrow 2Fe^{2+} + 6OH^- \tag{4}$$

Note that this autoreduction reaction generates OH^- and requires an electrolyte, such as NaCl, to be present in order to achieve local charge balance within the delamination. All three previous studies [9; 10; 25] were performed with such an electrolyte present. It would be necessary to perform additional experiments with DI water replacing the salt water in order to distinguish between these two mechanisms, although the Kelvin probe measurements of Andreon et al. [10] are suggestive that a form of cathodic delamination occurs, with the rate dictated by a tip autoreduction reaction.

5. CONCLUSIONS

The present approach uses a logical series of experiments to show that delamination of a MMA adhesive/steel sandwich panel occurs by water ingress, regardless of the presence or absence of oxygen or of an electrolyte. Broad conclusions are drawn without the use of a scanning Kelvin probe and chemical analysis. The operative delamination mechanism is labelled 'water attack'. However, the precise chemical reactions that give rise to the observed delamination have not been probed and are left for a future study.

- The insensitivity of delamination rate in steel/MMA/steel sandwich specimens to salt concentration (0 to 0.6 M NaCl) is strong evidence that cathodic delamination is inactive. The presence of the steel outer layers in the sandwich specimens starves the crack tip of oxygen. Consequently, the delamination rate is independent of the presence or absence of oxygen in the environment, implying that water attack occurs rather than free corrosion (or cathodic delamination).

- Water within the delamination attacks the crack tip region and leads to a delamination velocity that is independent of delamination length.

- Tests performed on coated steel specimens give additional support to water attack as a potential delamination mechanism: when oxygen is absent in these tests the delamination rate is the same as that observed in the sandwich specimens.

Acknowledgements

This research was carried out within the project "QUALIFY – Enabling Qualification of Hybrid Joints for Lightweight and Safe Maritime Transport", co-funded by the INTERREG 2SeasMers Zeeën programme http://www.interreg2seas.eu/qualify. The authors are grateful to Dr. Alessandro Leronni for insightful discussions.

Data availability

The raw/processed data required to reproduce these findings cannot be shared at this time due to technical or time limitations.

References

[1] S Askarinejad, E Martínez-Pañeda, II Cuesta, and N Fleck. Mode II fracture of an MMA adhesive layer: Theory versus experiment. *European Journal of Mechanics-A/Solids*, 86:104133, 2021.

[2] S Askarinejad, MD Thouless, and NA Fleck. Failure of a pre-cracked epoxy sandwich layer in shear. *European Journal of Mechanics-A/Solids*, 85:104134, 2021.

[3] RA Pethrick. Design and ageing of adhesives for structural adhesive bonding–A review. *Proceedings of the Institution of Mechanical Engineers, Part L: Journal of Materials: design and applications*, 229(5):349–379, 2015.

[4] AJ Kinloch. Interfacial fracture mechanical aspects of adhesive bonded joints—A review. *The Journal of Adhesion*, 10(3):193–219, 1979.

[5] R Posner, G Giza, M Marazita, and G Grundmeier. Ion transport processes at polymer/oxide/metal interfaces under varying corrosive conditions. *Corrosion science*, 52(5):1838–1846, 2010.

[6] A Nazarov, N Le Bozec, and D Thierry. Assessment of steel corrosion and deadhesion of epoxy barrier paint by scanning Kelvin probe. *Progress in Organic Coatings*, 114:123–134, 2018.

[7] HN McMurray and G Williams. Probe diameter and probe–specimen distance dependence in the lateral resolution of a scanning Kelvin probe. *Journal of Applied Physics*, 91(3):1673–1679, 2002.

[8] M Rohwerder and F Turcu. High-resolution Kelvin probe microscopy in corrosion science: scanning Kelvin probe force microscopy (skpfm) versus classical scanning Kelvin probe (skp). *Electrochimica Acta*, 53(2):290–299, 2007.

[9] JPB Van Dam, ST Abrahami, A Yilmaz, Y Gonzalez-Garcia, H Terryn, and JMC Mol. Effect of surface roughness and chemistry on the adhesion and durability of a

steel-epoxy adhesive interface. *International Journal of Adhesion and Adhesives*, 96:102450, 2020.

[10] B Andreon, BL Guenther, WL Cavalcanti, L Colombi Ciacchi, and P Plagemann. On the use of scanning kelvin probe for assessing in situ the delamination of adhesively bonded joints. *Corrosion Science*, 157:11–19, 2019.

[11] K Wapner, M Stratmann, and G Grundmeier. In situ infrared spectroscopic and scanning kelvin probe measurements of water and ion transport at polymer/metal interfaces. *Electrochimica Acta*, 51(16):3303–3315, 2006.

[12] JC Scully. *The Fundamentals of Corrosion*. Pergamon Press, Oxford, UK, 1966.

[13] M Stratmann, R Feser, and A Leng. Corrosion protection by organic films. *Electrochimica Acta*, 39(8-9):1207–1214, 1994.

[14] A Leng, H Streckel, and M Stratmann. The delamination of polymeric coatings from steel. part 1: Calibration of the kelvinprobe and basic delamination mechanism. *Corrosion Science*, 41(3):547–578, 1998.

[15] RG Schmidt and JP Bell. Epoxy adhesion to metals. In *Epoxy Resins and Composites II*, Advances in Polymer Science, vol 75, pages 33–71. Springer Berlin Heidelberg, 1986.

[16] RA Gledhill and AJ Kinloch. Environmental failure of structural adhesive joints. *The journal of adhesion*, 6(4):315–330, 1974.

[17] SYY Leung, DCC Lam, S Luo, and CP Wong. The role of water in delamination in electronic packages: degradation of interfacial adhesion. *Journal of adhesion science and technology*, 18(10):1103–1121, 2004.

[18] EL Koehler. The mechanism of cathodic disbondment of protective organic coatings—aqueous displacement at elevated pH. *Corrosion*, 40(1):5–8, 1984.

[19] A Leng, H Streckel, and M Stratmann. The delamination of polymeric coatings from steel. part 2: First stage of delamination, effect of type and concentration of cations on delamination, chemical analysis of the interface. *Corrosion Science*, 41(3):579–597, 1998.

[20] M Salerno and S Dante. Scanning Kelvin probe microscopy: Challenges and perspectives towards increased application on biomaterials and biological samples. *Materials*, 11(6):951, 2018.

[21] M Kendig, F Mansfeld, and S Tsai. Determination of the long term corrosion behavior of coated steel with ac impedance measurements. *Corrosion Science*, 23(4):317–329, 1983.

[22] A Leng, H Streckel, K Hofmann, and M Stratmann. The delamination of polymeric coatings from steel part 3: Effect of the oxygen partial pressure on the delamination reaction and current distribution at the metal/polymer interface. *Corrosion Science*, 41(3):599–620, 1998.

[23] N. Khayatan, A. C. A. de Vooys, and H. N. McMurray. The corrosion of chromium based coatings for packaging steel. *Electrochimica Acta*, 203:110311, 2016.

[24] S Pletincx, K Marcoen, L Trotochaud, L-L Fockaert, JMC Mol, AR Head, O Karslioglu, H Bluhm, Terryn H, and T Hauffman. Unravelling the chemical influence of water on the pmma/aluminium oxide hybrid interface in situ. *Scientific Reports*, 7:13341, 2017.

[25] PA Sørensen, K Dam-Johansen, CE Weinell, and S Kiil. Cathodic delamination of seawater-immersed anticorrosive coatings: Mapping of parameters affecting the rate. *Progress in Organic Coatings*, 68(4):283–292, 2010.

[26] N. Wint and M. Rohwerder. A new insight into the rate determining step of cathodic delamination. *Corrosion Science*, 202:326–336, 2022.

FIGURE CAPTIONS

Figure 1. Competing delamination mechanisms. (a) *Free corrosion* in which both half-reactions occur in close proximity, with ferrous ions and hydroxide ions combining to form hydrated rust. (b) *Cathodic delamination* in which oxygen reduction occurs at the crack tip, but iron oxidation occurs remotely from the delamination crack tip. The presence of sodium cations facilitates the production of OH^- anions at the crack tip which drive delamination; and (c) *Water attack* , regardless of whether oxygen is present or absent.

Figure 2. The manufacturing sequence of the MMA-coated steel specimens: (a) Mask with PTFE tape to induce the defect, (b) coat with MMA-Adhesive, (c) peel back adhesive, and (d) create an epoxy dam and fill defect with electrolyte.

Figure 3. (a) Specimen geometry and measurement of delamination length for the steel/MMA-adhesive/steel sandwich specimens. (b) Schematic of the MMA-coated steel substrate specimens with the adhesive covered by Al foil.

Figure 4. (a) Log-log plot of delamination length ℓ versus time t for a 100 µm thick MMA adhesive on a steel substrate, and exposed to 0.06 M, 0.6 M, and 3 M NaCl solutions and to de-ionised (DI) water. (b) Log-log plot of delamination length ℓ versus time t for steel/MMA-adhesive/steel sandwich specimens exposed to salt water (0.6 M NaCl solution) and to DI water in air, and in oxygen-starved environments. The slope is unity on the log-log plot, as indicated by the dotted line.

Figure 5. Delamination length ℓ versus time t for specimens immersed in DI water and in 0.6 M NaCl solution, for both steel/MMA adhesive/steel sandwich specimens and aluminium foil/MMA adhesive/steel specimens. To within the scatter of the data, the ℓ versus t characteristic is independent of the choice of top layer (steel sheet or aluminium foil), and of choice of environment (DI water or salt solution).

Figure 6. Delamination length ℓ versus time t for specimens comprising a 100 µm thick adhesive on steel substrate, with and without aluminium foil on the top surface of the adhesive, and exposed to 0.6 M NaCl solution or DI water. The data shown are

taken from Figs. 4 and 5.

Figure 7. Delamination length ℓ versus time t for a 100 µm thick adhesive layer on steel substrate exposed to 0.6 M NaCl and DI water. Measurements are shown for specimens in air and in oxygen-starved environments (200 mbar air or N_2 at 1 bar).

Figure 8. (a) A representative SEM micrograph of the surface of the as-received steel piece cleaned by acetone. SEM micrographs of the corroded surface of steel immersed in (b) 0.6 M NaCl solution and (c) DI water for 24 hours. SEM micrographs of the delaminated steel surface resulting from (d) cathodic delamination of an MMA-coated steel substrate immersed in 0.6 M NaCl solution, and (e) water attack of an MMA-coated steel substrate immersed in de-ionised water with oxygen absent. The images in (d) & (e) are 200 µm behind the delamination tip, and the arrow in each indicates the direction of delamination growth.

Figure 9. Delamination length ℓ versus time t for specimens of closed joint configuration. Data are taken from the literature and are compared to the results for steel/adhesive/steel sandwich specimens of the present study.

Table 1: Competing mechanisms of delamination

Mechanism	Fundamentals
A: Free corrosion	Production of both Fe^{2+} and OH^- at the crack tip. Needs O_2 supply.
B: Cathodic delamination	OH^- production at the delamination tip from O_2, Fe^{2+} production remotely, Na^+ diffuses within the delamination crack to give charge balance. Needs O_2 supply.
C: Water attack	Water molecules destroy the bond between steel and adhesive.

Table 2: Observable signatures for the competing mechanisms of delamination

Observable	Free corrosion	Cathodic delamination	Water attack
Sensitivity to concentration of Na^+ in H_2O	Low	High	Negligible
Sensitivity to availability of oxygen	High	High	Negligible
Fracture surface of steel substrate	Rusts & pits	Pristine	Pristine

Table 3: The sequence of experiments to identify the underlying corrosion mechanisms.

Test	Explore the sensitivity of delamination length ℓ to what?	Finding	Implication
Reference Expt. I	[NaCl]; MMA-coated steel in air.	$\ell(t)$ fast and sensitive to [NaCl], $\ell \propto t^{(1/2)}$, no rust.	Cathodic delamination, fed by oxygen through coating thickness and/or delamination.
Reference Expt. II	[NaCl]; steel/MMA/steel sandwich in air.	$\ell(t)$ slow and insensitive to [NaCl], $\ell \propto t$, no rust.	Water attack may occur as oxygen supply to delamination tip is limited.
Sensitivity Expt. III	Air or nitrogen environment; steel/MMA/steel sandwich with [NaCl] varied.	$\ell(t)$ slow and insensitive to [NaCl] and the delamination grows at the same rate in both air and nitrogen. $\ell \propto t$, no rust.	Water attack may occur in air, as oxygen supply to delamination tip is limited. Water attack also occurs in nitrogen.
Sensitivity Expt. IV	Bending stiffness of substrate; replace one steel shim by a thin Al layer. Air environment with [NaCl] varied.	$\ell(t)$ slow and insensitive to bending stiffness of substrate and insensitive to [NaCl], $\ell \propto t$, no rust.	Cathodic delamination of coated steel is due to oxygen supply through thickness of MMA-coating, and not due to oxygen supply along delamination.
Sensitivity Expt. V	$[O_2]$ in MMA-coated steel; [NaCl] varied.	$\ell(t)$ sensitive to $[O_2]$ and $\ell \propto t^{(1/2)}$ and fast when $[O_2]$ and [NaCl] are high. Otherwise, $\ell \propto t$ and slow.	MMA-coated steel, with oxygen absent, delaminates by water attack, and mimics steel/MMA/steel sandwich in air.

Key: [X] denotes concentration of species X.

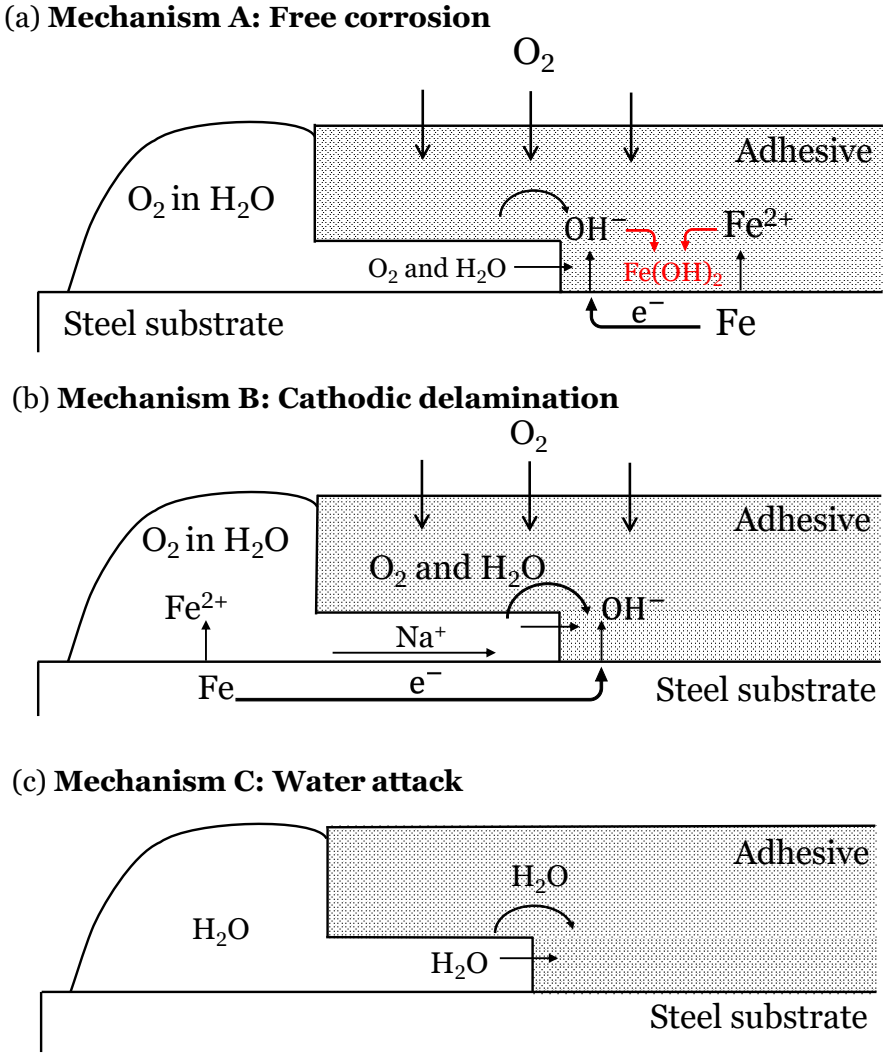

Figure 1: Competing delamination mechanisms. (a) *Free corrosion* in which both half-reactions occur in close proximity, with ferrous ions and hydroxide ions combining to form hydrated rust. (b) *Cathodic delamination* in which oxygen reduction occurs at the crack tip, but iron oxidation occurs remotely from the delamination crack tip. The presence of sodium cations facilitates the production of OH^- anions at the crack tip which drive delamination; and (c) *Water attack*, regardless of whether oxygen is present or absent.

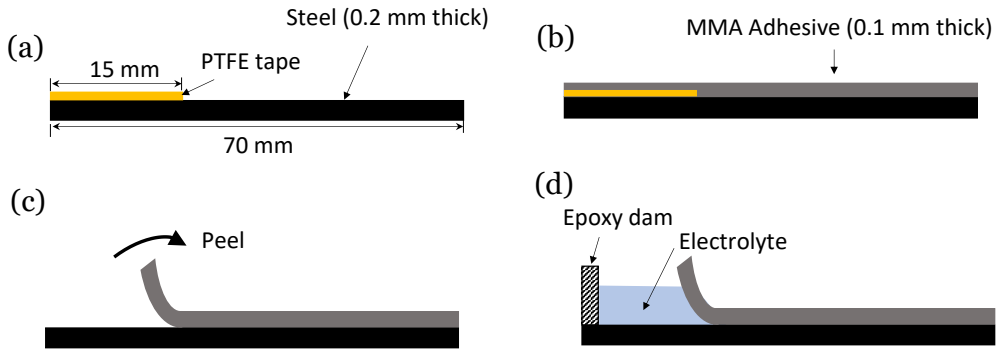

Figure 2: The manufacturing sequence of the MMA-coated steel specimens: (a) Mask with PTFE tape to induce the defect, (b) coat with MMA-Adhesive, (c) peel back adhesive, and (d) create an epoxy dam and fill defect with electrolyte.

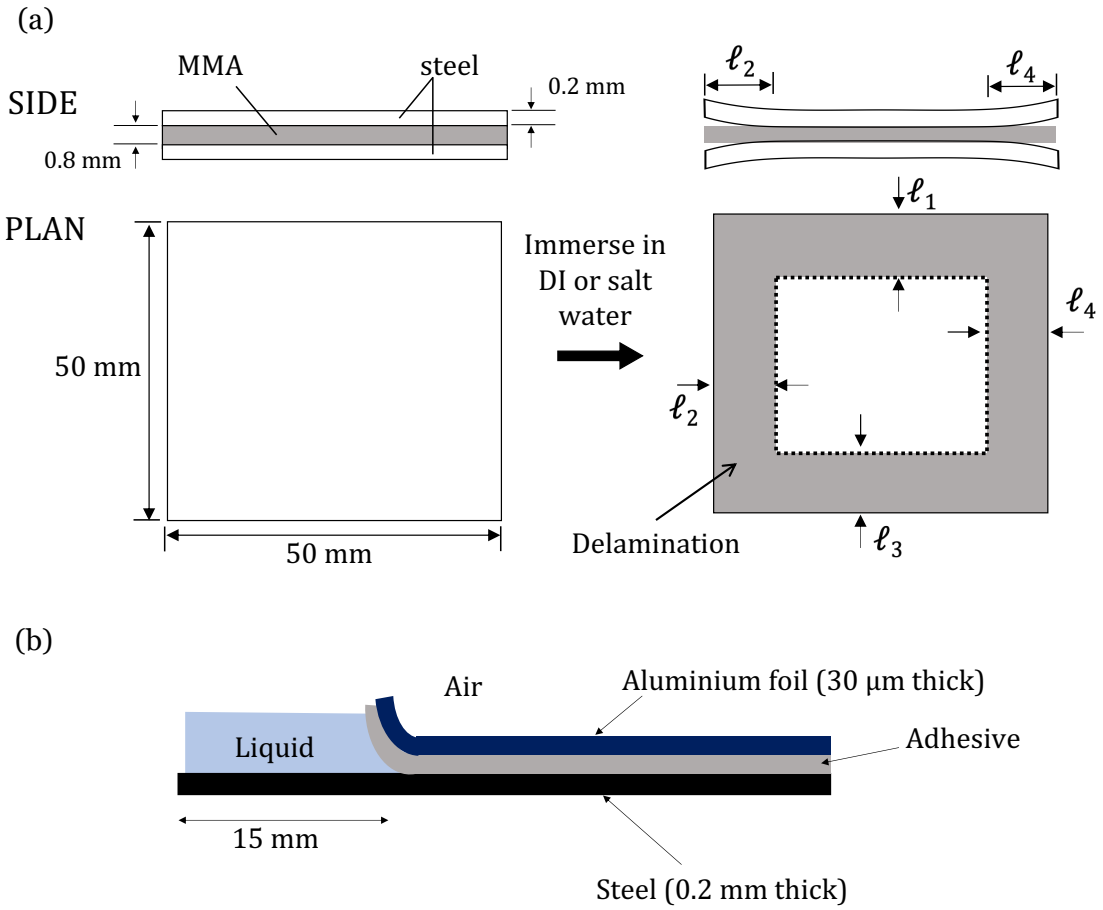

Figure 3: (a) Specimen geometry and measurement of delamination length for the steel/MMA-adhesive/steel sandwich specimens. (b) Schematic of the MMA-coated steel substrate specimens with the adhesive covered by Al foil.

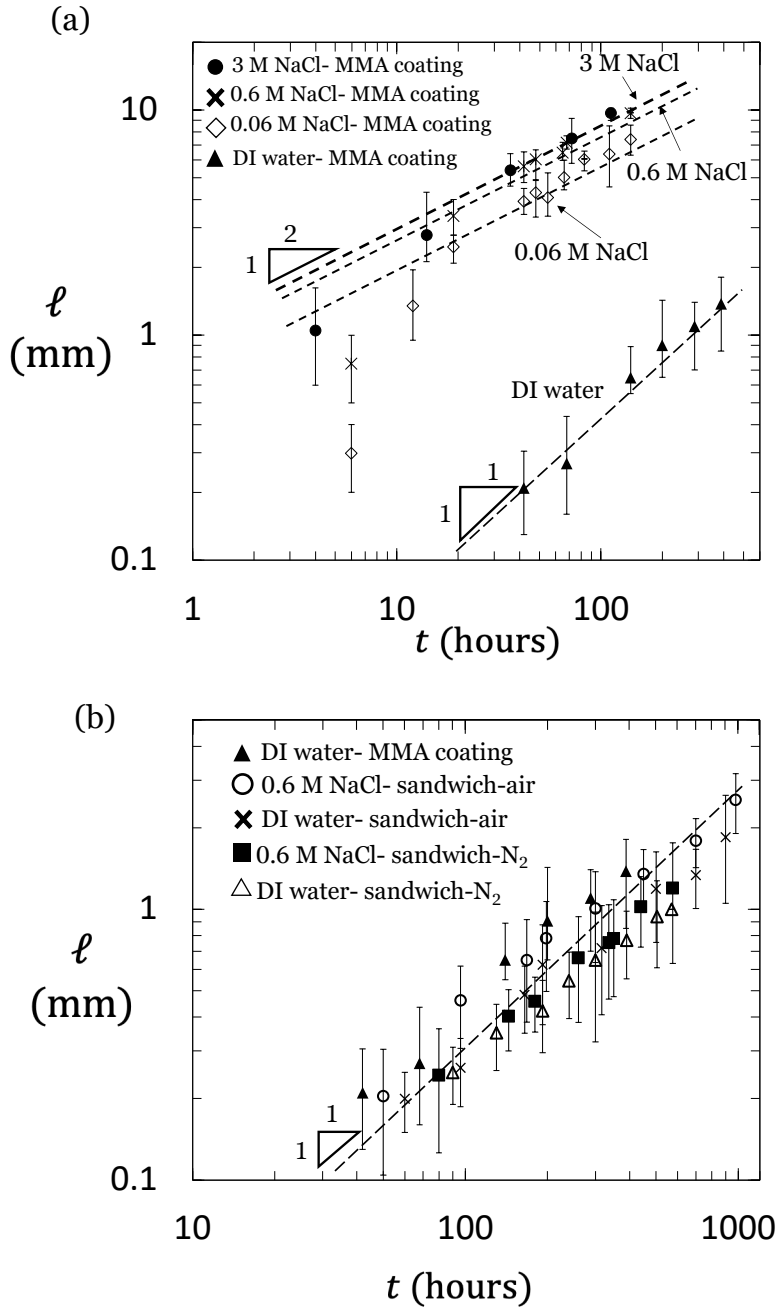

Figure 4: (a) Log-log plot of delamination length ℓ versus time t for a 100 µm thick MMA adhesive on a steel substrate, and exposed to 0.06 M, 0.6 M, and 3 M NaCl solutions and to de-ionised (DI) water. (b) Log-log plot of delamination length ℓ versus time t for steel/MMA-adhesive/steel sandwich specimens exposed to salt water (0.6 M NaCl solution) and to DI water in air, and in oxygen-starved environments. The slope is unity on the log-log plot, as indicated by the dotted line.

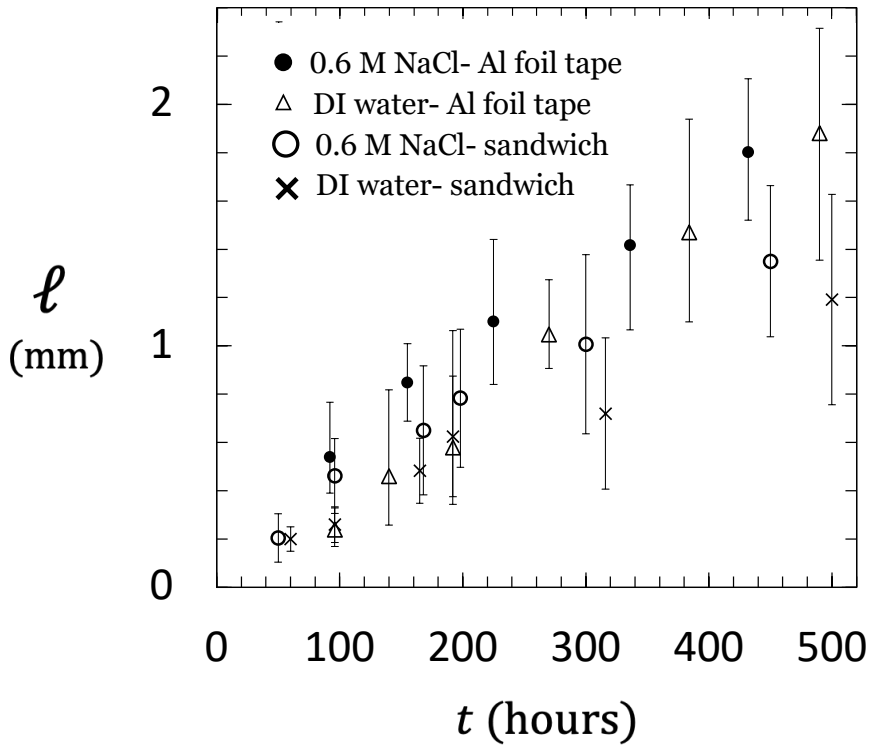

Figure 5: Delamination length ℓ versus time t for specimens immersed in DI water and in 0.6 M NaCl solution, for both steel/MMA adhesive/steel sandwich specimens and aluminium foil/MMA adhesive/steel specimens. To within the scatter of the data, the ℓ versus t characteristic is independent of the choice of top layer (steel sheet or aluminium foil), and of choice of environment (DI water or salt solution).

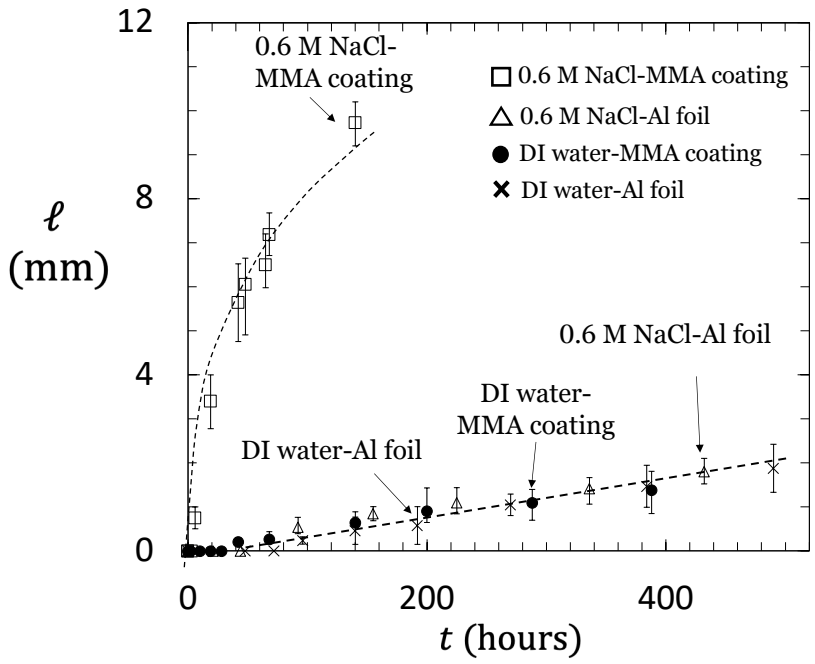

Figure 6: Delamination length ℓ versus time t for specimens comprising a 100 µm thick adhesive on steel substrate, with and without aluminium foil on the top surface of the adhesive, and exposed to 0.6 M NaCl solution or DI water. The data shown are taken from Figs. 4 and 5.

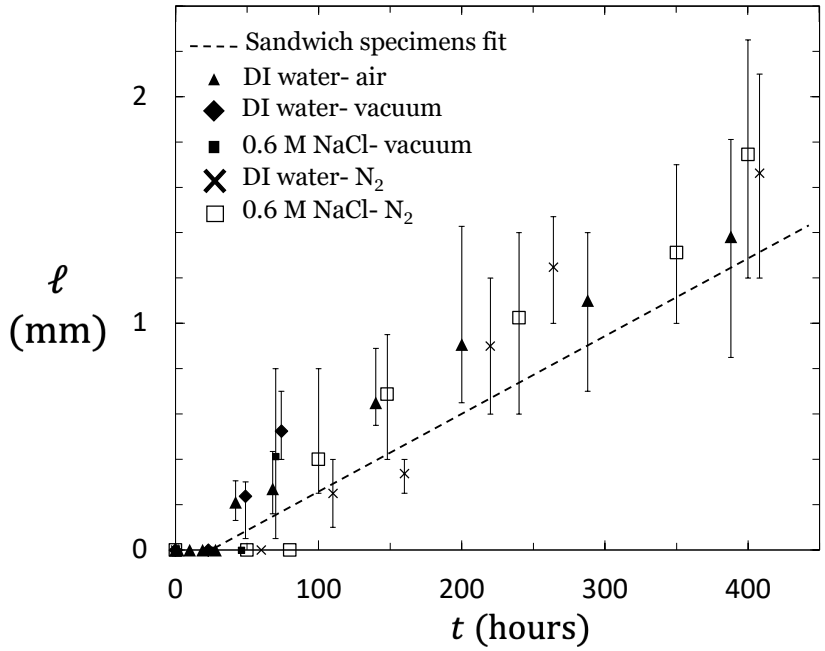

Figure 7: Delamination length ℓ versus time t for a 100 µm thick adhesive layer on steel substrate exposed to 0.6 M NaCl and DI water. Measurements are shown for specimens in air and in oxygen-starved environments (200 mbar air or N_2 at 1 bar).

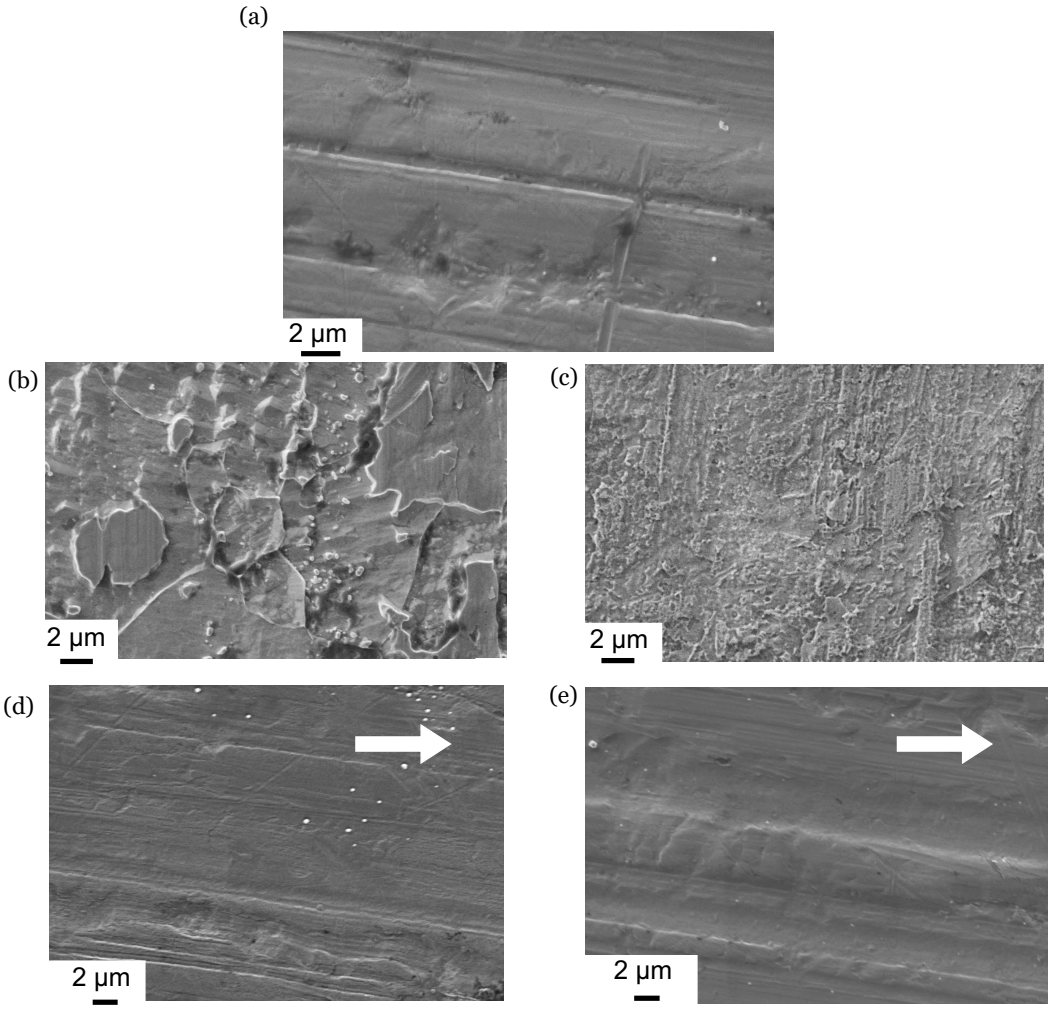

Figure 8: (a) A representative SEM micrograph of the surface of the as-received steel piece cleaned by acetone. SEM micrographs of the corroded surface of steel immersed in (b) 0.6 M NaCl solution and (c) DI water for 24 hours. SEM micrographs of the delaminated steel surface resulting from (d) cathodic delamination of an MMA-coated steel substrate immersed in 0.6 M NaCl solution, and (e) water attack of an MMA-coated steel substrate immersed in de-ionised water with oxygen absent. The images in (d) & (e) are 200 µm behind the delamination tip, and the arrow in each indicates the direction of delamination growth.

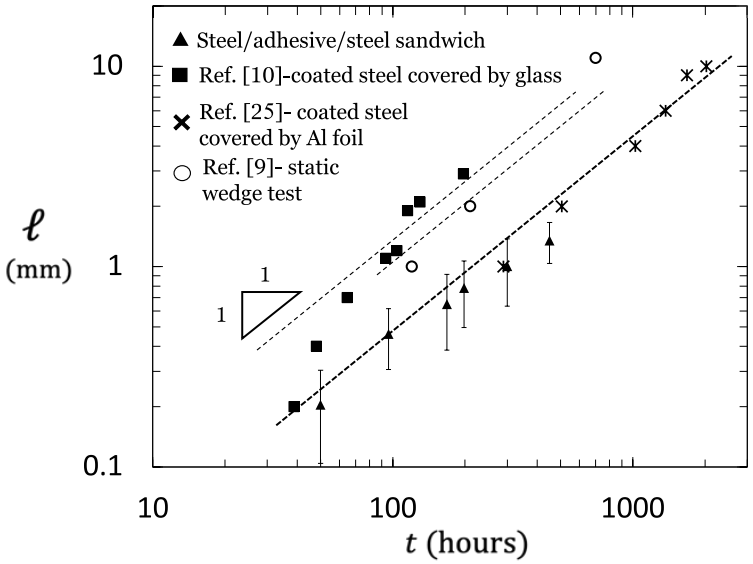

Figure 9: Delamination length ℓ versus time t for specimens of closed joint configuration. Data are taken from the literature and are compared to the results for steel/adhesive/steel sandwich specimens of the present study.